

Unlock your experimental potential
with power and agility
BD FACSymphony™ A5 SE Cell Analyzer
Discover the difference >



PU.1 Regulates Ig Light Chain Transcription and Rearrangement in Pre-B Cells during B Cell Development

This information is current as
of February 26, 2022.

Carolina R. Batista, Stephen K. H. Li, Li S. Xu, Lauren A. Solomon and Rodney P. DeKoter

J Immunol 2017; 198:1565-1574; Prepublished online 6
January 2017;

doi: 10.4049/jimmunol.1601709

<http://www.jimmunol.org/content/198/4/1565>

Supplementary Material <http://www.jimmunol.org/content/suppl/2017/01/06/jimmunol.1601709.DCSupplemental>

References This article **cites 54 articles**, 22 of which you can access for free at:
<http://www.jimmunol.org/content/198/4/1565.full#ref-list-1>

Why *The JI*? Submit online.

- **Rapid Reviews! 30 days*** from submission to initial decision
- **No Triage!** Every submission reviewed by practicing scientists
- **Fast Publication!** 4 weeks from acceptance to publication

**average*

Subscription Information about subscribing to *The Journal of Immunology* is online at:
<http://jimmunol.org/subscription>

Permissions Submit copyright permission requests at:
<http://www.aai.org/About/Publications/JI/copyright.html>

Email Alerts Receive free email-alerts when new articles cite this article. Sign up at:
<http://jimmunol.org/alerts>



PU.1 Regulates Ig Light Chain Transcription and Rearrangement in Pre-B Cells during B Cell Development

Carolina R. Batista,^{*,†,‡} Stephen K. H. Li,^{*,†} Li S. Xu,^{*,†,‡} Lauren A. Solomon,^{*,†,‡} and Rodney P. DeKoter^{*,†,‡}

B cell development and Ig rearrangement are governed by cell type- and developmental stage-specific transcription factors. PU.1 and Spi-B are E26-transformation-specific transcription factors that are critical for B cell differentiation. To determine whether PU.1 and Spi-B are required for B cell development in the bone marrow, *Spi1* (encoding PU.1) was conditionally deleted in B cells by Cre recombinase under control of the *Mb1* gene in *SpiB* (encoding Spi-B)-deficient mice. Combined deletion of *Spi1* and *SpiB* resulted in a lack of mature B cells in the spleen and a block in B cell development in the bone marrow at the small pre-B cell stage. To determine target genes of PU.1 that could explain this block, we applied a gain-of-function approach using a PU.1/Spi-B-deficient pro-B cell line in which PU.1 can be induced by doxycycline. PU.1-induced genes were identified by integration of chromatin immunoprecipitation-sequencing and RNA-sequencing data. We found that PU.1 interacted with multiple sites in the *Igκ* locus, including *Vκ* promoters and regions located downstream of *Vκ* second exons. Induction of PU.1 induced *Igκ* transcription and rearrangement. Upregulation of *Igκ* transcription was impaired in small pre-B cells from PU.1/Spi-B-deficient bone marrow. These studies reveal an important role for PU.1 in the regulation of *Igκ* transcription and rearrangement and a requirement for PU.1 and Spi-B in B cell development. *The Journal of Immunology*, 2017, 198: 1565–1574.

B cell development involves ordered rearrangement of *Ig* loci encoding H and L chain proteins that assemble into Abs capable of recognizing specific Ags. Stages of B cell development can be resolved using cell surface marker expression, as well as *Ig* gene rearrangement (1–3). Progenitor B (pro-B; also known as pre-BI) cells are generated from lymphoid progenitors and initiate *D-J* segment rearrangement of *Igh* H chain alleles. Rearrangement of *Igh* alleles is completed by *V-DJ* rearrangement to encode H chains that can pair with surrogate L chain proteins and be deposited on the cell surface as a pre-BCR. Pre-BCR signaling promotes proliferation of large pre-B cells (also known

as pre-BII cells). Cessation of proliferation induces re-expression of the RAG proteins RAG1 and RAG2, whose interaction is widespread throughout the *Ig* loci at recombination signal sequences (RSSs) (4). Finally, successful pairing of *Igκ* or *λ* L chain proteins with *IgH* proteins results in expression of a BCR in immature B cells (5). Immature B cells emigrate from the bone marrow (BM) to the spleen to complete their maturation (6).

The mouse *Igκ* locus contains 101 functional *Vκ* genes, 60 *Vκ* pseudogenes, 4 functional *Jκ* genes, 1 *J* pseudogene, and 1 *Cκ* gene (7, 8). The *Igκ* locus comprises >3 MB of genomic sequence (8). Recombination occurs in a developmental stage-specific order that is thought to be regulated at the level of chromatin accessibility to RAG proteins (7, 9). Accessibility is likely controlled at the level of transcription, as supported by two lines of evidence. First, deletions of enhancers within the *Igκ* locus impair transcription and *Ig* recombination (10, 11). Second, deletion of genes encoding histone-modifying enzymes or transcription factors reduce transcription and *Ig* recombination (8). Thus, *Ig* locus accessibility is regulated by transcription factor recruitment of the transcriptional machinery to regulatory regions within the *Igκ* locus.

B cell development is coordinated by the expression of a number of cell type- and developmental stage-specific transcription factors, including E2A, EBF, Pax5, Ikaros, PU.1, and Spi-B (12). PU.1 (encoded by *Spi1*) and Spi-B (encoded by *SpiB*) are highly related transcription factors of the E26 transformation-specific (ETS) family (13). Several lines of evidence suggest that PU.1 might play an important role in the control of *Igκ* transcription. *Igκ* V region promoters, as well as the intronic and 3' enhancers in the *Igκ* locus, contain predicted binding sites for PU.1 (14–16). Chromatin immunoprecipitation-sequencing (ChIP-seq) analysis in pro-B cells reveals that PU.1 binding is widespread throughout the *Igκ* locus (8, 17). However, there has not been a clear demonstration of a role for PU.1 in *Ig* transcription, accessibility, or rearrangement in vivo. The ability of Spi-B to complement PU.1 function may have impeded a clear demonstration of PU.1 as a regulator of *Igκ* gene transcription (13, 18). We previously

*Department of Microbiology and Immunology, Schulich School of Medicine and Dentistry, Western University, London, Ontario N6A 5C1, Canada; [†]The Centre for Human Immunology, Schulich School of Medicine and Dentistry, Western University, London, Ontario N6A 5C1, Canada; and [‡]Division of Genetics and Development, Children's Health Research Institute, Lawson Research Institute, London, Ontario N6C 2R5, Canada

ORCID: 0000-0002-0236-3273 (S.K.H.L.).

Received for publication October 4, 2016. Accepted for publication December 12, 2016.

This work was supported by Ontario Trillium (to C.R.B.), the Leukemia and Lymphoma Society of Canada (to R.P.D.), and by Canadian Institutes of Health Research Grants MOP-10651 and MOP-137414 (to R.P.D.).

Chromatin immunoprecipitation-sequencing and RNA-sequencing data presented in this article have been submitted to the Gene Expression Omnibus (<https://www.ncbi.nlm.nih.gov/geo/>) under accession number GSE87316.

Address correspondence and reprint requests to Dr. Rodney P. DeKoter, Department of Microbiology and Immunology, Schulich School of Medicine and Dentistry, Western University, Dental Sciences 3007, London, ON N6A 5C1, Canada. E-mail address: rdekoter@uwo.ca

The online version of this article contains supplemental material.

Abbreviations used in this article: ΔB, *Mb1*^{+/+} *Spi1*^{+/+} *SpiB*^{-/-}; BM, bone marrow; ChIP, chromatin immunoprecipitation; ChIP-seq, chromatin immunoprecipitation-sequencing; DAVID, Database for Annotation, Visualization and Integrated Discovery; EICE, ETS-IRF composite element; ETS, E26 transformation-specific; *Mb1*-CreΔP, *Mb1*^{+/Cre} *Spi1*^{lox/lox} *SpiB*^{+/+}; *Mb1*-CreΔPB, *Mb1*^{+/Cre} *Spi1*^{lox/lox} *SpiB*^{-/-}; pro-B, progenitor B; RNA-seq, RNA-sequencing; RSS, recombination signal sequence; RT-qPCR, quantitative RT-PCR; TSS, transcription start site; WT, wild-type.

Copyright © 2017 by The American Association of Immunologists, Inc. 0022-1767/17/\$30.00

generated mice that delete *Spi1* encoding PU.1 under control of CD19-Cre on a *Spi1*^{-/-} background (18). These mice had impaired development of follicular B cells and perturbation of BM B cell development, demonstrating a complementary role for PU.1 and Spi-B in B cell development and function (18, 19). However, CD19-Cre does not delete alleles efficiently in BM (20), precluding an examination of PU.1 and Spi-B function in early B cell development. We hypothesized that deletion of *Spi1* and *SpiB* during early B cell development would reveal a role for PU.1 and/or Spi-B in the transcription and rearrangement of *Ig* genes.

To test this hypothesis, *Mb1*^{+Cre} *Spi1*^{lox/lox} *SpiB*^{-/-} (*Mb1*-CreΔPB) mice were generated by crossing *Spi1*^{lox/lox} *SpiB*^{-/-} mice to *Mb1*^{+Cre} mice. *Mb1*-Cre deletes alleles with high efficiency in BM (20), resulting in a *SpiB*-deficient mouse that is expected to have a high frequency of *Spi1* deletion during early B cell development. Analysis of adult mice showed that deletion of *Spi1* and *SpiB* in *Mb1*-CreΔPB mice resulted in the absence of IgM⁺ B cells in the spleen. In BM, there was a specific block in B cell development at the small pre-B cell to immature B cell transition that is marked by successful rearrangement of *Ig* L chain genes. To determine target genes of PU.1 that could explain this block, we applied a gain-of-function approach using a PU.1/Spi-B-deficient pro-B cell line in which PU.1 can be induced by doxycycline. PU.1-regulated genes were identified by integration of ChIP-seq and RNA-sequencing (RNA-seq) data. PU.1 interacted with 23,647 sites located near transcription start sites (TSSs) of genes involved in immune system development. Interestingly, we observed PU.1 interaction with multiple sites in *Vκ* gene promoters, as well as sites downstream of *Vκ* second exons located near RSSs. Induction of PU.1 resulted in increased transcription of *Igκ* V genes and *Igκ* rearrangement. Finally, we found that upregulation of *Igκ* transcription was impaired in PU.1 and Spi-B-deficient BM pre-B cells. These studies reveal an important role for PU.1 in *Igκ* transcription and rearrangement and a requirement for PU.1 and Spi-B in B cell development.

Materials and Methods

Mice

Mb1-Cre mice were described previously (20). *Mb1*-Cre mice were crossed with *Spi1*^{lox/lox} *SpiB*^{-/-} to generate *Mb1*-CreΔPB mice. *Mb1*^{+Cre} *Spi1*^{lox/lox} *SpiB*^{+/+} (*Mb1*-CreΔP) and *Mb1*^{+Cre} *Spi1*^{+/+} *SpiB*^{-/-} or *Mb1*^{+/+} *Spi1*^{+/+} *SpiB*^{-/-} (ΔB) mice were used as experimental controls. C57BL/6 mice were purchased from Charles River Laboratories (Saint-Constant, QC, Canada). All experiments were performed in compliance with the Western University Council on Animal Care.

Flow cytometry and cell sorting

For spleen and BM analysis, cells were prepared from 6–10-wk-old *Mb1*-CreΔPB, *Mb1*-CreΔP, ΔB, and wild-type (WT) mice. RBCs were removed from single-cell suspensions using hypotonic lysis. Flow cytometric analyses were performed using an LSR II instrument (BD Immunocytometry Systems, San Jose, CA). Abs were purchased from eBioscience (San Diego, CA), BioLegend (San Diego, CA), or BD Biosciences (Mississauga, ON, Canada) and included PE-anti-CD19 (1D3), FITC-anti-BP-1 (6C3), allophycocyanin-anti-B220 (RA3-6B2), allophycocyanin-anti-IgM (II/41), PE-anti-Igκ (187.1), FITC-anti-IL-7R (A7R34), BV421-anti-B220 (RA3-6B2), PE-anti-BP-1 (6C3), FITC-anti-CD24 (M1/69), biotin-anti-CD43 (S7), and PE/Cy5 streptavidin. BM cell sorting was performed on a FACSAria with FACSDiva software (both from BD). Data were analyzed using FlowJo 9.7.4 software.

Cell culture

The 660BM and i660BM cell lines used in this study were described previously (19). Cells were cultured in IMDM (Wisent, QC, Canada) containing 5% IL-7-conditioned medium from the J558L-IL-7 cell line (21), 10% FBS (Wisent), 1× penicillin/streptomycin/L-glutamine (Lonza, Shawinigan, QC, Canada), and 5 × 10⁻⁵ M 2-ME (Sigma-Aldrich, St. Louis, MO). i660BM cells were maintained in 0.5 μg/ml puromycin

(BioBasic, Markham, ON, Canada). Cell lines were maintained in 5% CO₂ atmosphere at 37°C.

RNA-seq analysis

i660BM cells were induced for 48 h with doxycycline (70 ng/μl) in the presence of 5% IL-7-conditioned medium described above, and RNA was extracted using an RNeasy Kit (QIAGEN, ON, Canada). Uninduced cells were used as a control. Paired-end (mRNA-sequencing stranded) libraries were prepared using Illumina TrueSeq Adapters. Libraries were sequenced using an Illumina HiSeq2000 sequencer in paired-end mode. Data analysis was performed as described previously (22) using the tools available in Galaxy suite (23). Standard Illumina sequencing adaptors (5'-AGATCGGAAGAGC-3') and short reads were removed using Trim Galore! V0.2.8.1 in mate-paired mode with trim low quality: 20; maximum allowed error rate: 0.1; discard reads that became shorter than length: 20. Trimmed FASTQ files were aligned to the mouse genome (mm10) using TopHat2 v2.0.9 in mate-paired mode, with mean inner distance between mate pairs: 140 and SD for distance between mate pairs: 30. Assembled transcript abundance and differential gene expression were determined using Cufflinks/Cuffdiff v2.1.1. Reference annotation files were downloaded from UCSC RefSeq Genes (GRCm38/mm10) in gtf format. Cuffdiff output genes with a fold change > 0.5 or < 0.5 (log₂) were classified as significantly upregulated or downregulated genes, respectively. Transcripts presenting PU.1 ChIP peaks within 15 kb upstream or downstream of the TSS and exhibiting significant fold change by RNA-seq were considered PU.1-regulated genes. Functional classification analysis was performed on predicted PU.1 target genes from the Database for Annotation, Visualization and Integrated Discovery (DAVID) using GOTERM_BP_FAT (24). Functional protein classification of PU.1-regulated genes was determined using the PANTHER classification system (25).

ChIP and ChIP-seq analysis

i660BM cells were induced for 24 h with doxycycline (70 ng/μl) in the presence of 5% IL-7-conditioned medium described above. Chromatin was cross-linked with 1% paraformaldehyde for 10 min, and cross-linking was terminated by the addition of glycine. Chromatin yielding 150–300 μg was immunoprecipitated using Dynabeads Protein G (Life Technologies) conjugated to 6 μg of rabbit polyclonal anti-PU.1 Ab (Santa Cruz Biotechnology, Santa Cruz, CA) or 6 μg of rabbit polyclonal anti-IgG Ab (Abcam, ON, Canada). Immunoprecipitated chromatin was de-cross-linked and DNA was purified using a QIAquick PCR Purification Kit (QIAGEN). PU.1 immunoprecipitation was validated by quantitative RT-PCR (RT-qPCR) using two sets of primers for the *E2f1* gene: a positive set targeting the PU.1 binding site on intron 1 of the *E2f1* gene and a negative set targeting a region on intron 4 of the *E2f1* gene. Illumina TruSeq DNA libraries were prepared from two biological replicates of PU.1-immunoprecipitated chromatin and one sample of input chromatin. Libraries were sequenced using an Illumina HiSeq2000 SR100 sequencer (Génome Québec Innovation Centre, QC, Canada). ChIP-seq data analysis was conducted using Galaxy Suite (23). Illumina sequencing adaptors were removed using Trim Galore! Trimmed FASTQ files were aligned to the mouse reference genome GRCm38/mm10 with Bowtie, reporting only the best alignment for each fragment (–best) with a maximum number of two mismatches with an average quality score ≥ 70 (26). Experimental replicate BAM aligned files were merged using merge BAM files in Galaxy. Peaks were called using MACS1.4.1 with a mappable genome size of 1.8 × 10¹⁰ bp (mm10). Peaks were called with a tag size to 100, bandwidth of 300, and a *p* value cutoff for peak detection of 1e–07. Sequences of regions with significant PU.1 binding were extracted using extract genomic DNA in Galaxy. Motif discovery was performed with MEME-CHIP version 4.11.1. Functional analysis of *cis*-regulatory regions bound by PU.1 were identified using CEAS (27). Heat maps of ChIP signals surrounding TSSs were generated using deepTools2 (28).

Igκ locus analysis

Transcription of *Igκ* genes was evaluated from RNA-seq data using Cufflinks and the GENCODE mouse reference that contains a complete annotation for the *Ig* gene segments (29). Average fold change expression of *Igκ* genes was determined from three replicates for each group (–DOX and +DOX). *Igκ* genes were classified as upregulated (fold change > 1.0) or downregulated (fold change < –1.0) as a ratio between induced and control condition. A heat map illustrating the upregulated and downregulated genes was generated using GENE-E (Broad Institute, Cambridge, MA). Regions of PU.1 binding were intersected with the reference vM9 GENCODE to correlate ChIP binding with transcripts using bedtools

v2.22.1 (30). Regions overlapping by ≥ 1 bp were reported as PU.1-bound transcripts and presented as Venn diagrams generated using InteractiVenn (31). RNA-seq and ChIP-seq genome tracks were visualized in the UCSC genome browser.

PCR and gene-expression analysis

Genomic DNA was prepared from 660BM or i660BM cells after 48 h of PU.1 induction with doxycycline (70 ng/ μ l) with low (0.1 ng/ μ l) or high (7.5 ng/ μ l) IL-7. RNA was prepared using TRIzol Reagent or an AllPrep DNA/RNA Mini Kit (QIAGEN) from 660BM or i660BM cells after 48 h of PU.1 induction with doxycycline (70 ng/ μ l) in 5 or 2.5% IL-7-conditioned medium. cDNA was synthesized from purified RNA using an iScript cDNA synthesis kit (Bio-Rad). cDNA was diluted to a concentration of 30 ng/ μ l in RNase-free water for the RT-qPCR reactions. PCR reactions to detect *Igk* rearrangements were performed as previously described (32). RT-qPCR reactions were prepared with specific primers for the genes of interest using SensiFAST SYBR green (BioLine, London, U.K.), and amplification was performed on a Rotor Gene 6000 instrument (Corbett Life Sciences, Valencia, CA). Gene expression was normalized to *B2m* expression, and fold expression was calculated using the Δ threshold cycle method (33). Primer sequences are shown in Supplemental Table I.

Statistical analysis

All data are graphed as mean \pm SEM. Statistical analysis was performed with Prism 5.0 (GraphPad, La Jolla, CA) using ANOVA or the Student *t* test, as appropriate. The *p* values ≤ 0.05 were considered significant.

Availability of data

ChIP-seq and RNA-seq data have been submitted to the Gene Expression Omnibus (<https://www.ncbi.nlm.nih.gov/geo/>) under accession number GSE87316.

Results

Deletion of genes encoding PU.1 and Spi-B impairs B cell development at the pre-B to immature B cell transition

It was shown that mice lacking PU.1 or Spi-B in the B cell lineage have relatively normal B cell development and mild impairment of B cell function (34–36). However, mice lacking PU.1 and Spi-B in the B cell lineage (*Cd19^{Cre} Spi1^{lox/lox} SpiB^{-/-}* mice) have reduced numbers of B cells, suggesting that these factors are important during development (18, 19). We sought to determine whether efficient deletion of PU.1 and Spi-B in the early stages of B cell development in BM would result in a block at a specific stage. Mice that delete *Spi1* under control of the *Cd79a* (Mb-1) gene, which deletes alleles efficiently in BM (20), were bred to *SpiB^{-/-}* mice to generate Mb1-Cre Δ PB mice (lacking PU.1 and Spi-B), Mb1-Cre Δ P mice (lacking PU.1), and Δ B mice (lacking Spi-B). To assess B cell development, the frequency of mature B cells in the spleen of 6–10 wk old mice was determined. Mb1-Cre Δ PB mice had few B220⁺ IgM⁺ B cells in the spleen compared with WT or Δ B mice (Fig. 1). Therefore, PU.1 and Spi-B are required to generate splenic B cells. To determine the stage at which the block of B cell development was occurring, the frequencies of developing B cells in BM of 6–10-wk-old Mb1-Cre Δ PB mice were measured using flow cytometry according to the cell surface marker scheme described by Hardy et al. (3). There were no significant differences in the frequencies of B220⁺ cells among the groups (Fig. 2A, 2B). However, immature BM B cells (B220⁺ CD43⁺) were increased in frequency and mature BM B cells (B220⁺ CD43⁻) were decreased in frequency in Mb1-Cre Δ PB mouse BM compared with Mb1-Cre Δ P, Δ B, and WT mouse BM (Fig. 2C–E). As a proportion of total B220⁺ cells, there were reduced frequencies of cells at the pre-pro B cell stage, or fraction A, in Mb1-Cre Δ PB, Mb1-Cre Δ P, and Δ B mice compared with WT mice (Fig. 2F, 2G). There were increased frequencies of fraction B (pro-B/pre-BI) cells and fraction C (pre-B, large pre-B/pre-BII) cells in Mb1-Cre Δ PB mouse BM compared with controls (Fig. 2F, 2G). Mb1-Cre Δ P mice had double the frequency of

fraction C BM cells compared with controls (Fig. 2F, 2G). None of the groups analyzed showed significant differences in the frequencies of fraction D (small pre-B) cells. However, fraction E (immature B cells) and fraction F (mature recirculating B cells) were nearly absent in Mb1-Cre Δ PB BM. Strikingly, there were no B cells expressing high levels of surface Ig in 6–10-wk-old Mb1-Cre Δ PB mice (Fig. 2F, 2G). These results demonstrate a critical requirement for PU.1 and Spi-B in the transition from small pre-B cells to immature B cells.

Analysis of PU.1 target genes in the pro-B cell line i660BM

To identify target genes of PU.1 that could explain the developmental block in Mb1-Cre Δ PB mouse BM, we applied a gain-of-function approach using a PU.1-inducible pro-B cell line (Fig. 3A). The 660BM cell line is fully deleted for *Spi1* and *SpiB*, has a nonproductive rearrangement of the *Igh* locus, and is germline for *Igk* locus rearrangement (19) (data not shown). The i660BM cell line is infected with a two-vector inducible system in which PU.1 is inducible using 70 ng/ml doxycycline (19). To define sites of PU.1 interaction, anti-PU.1 ChIP was performed on chromatin prepared from i660BM cells induced with (+DOX) or without (–DOX) 70 ng/ml doxycycline for 24 h. Illumina sequencing was performed on two biological replicates of PU.1-induced chromatin, as well as input chromatin. An average of 70 million 100-bp single-end reads were obtained. Reads were aligned to the mouse genome (mm10), and data were analyzed using the Galaxy suite of software tools. PU.1 was found to be associated with 49,385 unique genomic regions. The top interaction motif recovered for all PU.1-associated regions was the ETS motif containing the core A/5'-GGAA-3' sequence (Fig. 3B). PU.1 was found to associate primarily with distal intergenic regions and gene bodies, similar to what was reported previously for PU.1 in splenic B cells (Fig. 3C) (37). Seventeen percent of PU.1-interaction sites were at annotated gene promoters, and 23,647 peaks were located within 15 kb of annotated TSSs (Fig. 3C, 3D).

Next, RNA-seq analysis was performed on three biological replicates of RNA prepared from i660BM cells induced or not with 70 ng/ml doxycycline for 48 h. An average of 60 million 100-bp paired-end reads were obtained per sample. RNA-seq reads were aligned to the mouse genome (mm10) using TopHat, and differential gene expression was determined using Cufflinks suite. Genes presenting a log₂-fold change in expression > 0.5 were considered in our analysis. Using these criteria, transcript levels of 811 genes were significantly increased upon PU.1 induction, and transcript levels of 531 genes were significantly decreased upon PU.1 induction (Supplemental Table II).

To identify PU.1-regulated genes, the genomic region that interacts with PU.1 was associated with differentially expressed transcripts. A total of 793 of 811 upregulated genes and 521 of 531 downregulated genes were associated with PU.1 binding sites located within 15 kb of the TSS, suggesting that these genes were regulated directly by PU.1 (Fig. 3E). As shown in Fig. 3F, 670 PU.1-associated genes were upregulated and 465 PU.1-associated genes were downregulated with fold changes in expression $< \log_2$ (1.5). However, 141 genes were upregulated $> \log_2$ (1.5)-fold, of which 12 were upregulated $> \log_2$ (5)-fold. Sixty-six genes were downregulated $> \log_2$ (1.5)-fold, of which five were downregulated $> \log_2$ (3)-fold (Fig. 3F). In summary, 793 upregulated gene transcripts and 521 downregulated gene transcripts were associated with PU.1 peaks and, therefore, were considered direct targets of PU.1 regulation.

Gene ontology analysis of PU.1 targets

Upregulated and downregulated genes associated with PU.1 binding in i660BM cells were explored further using gene ontology

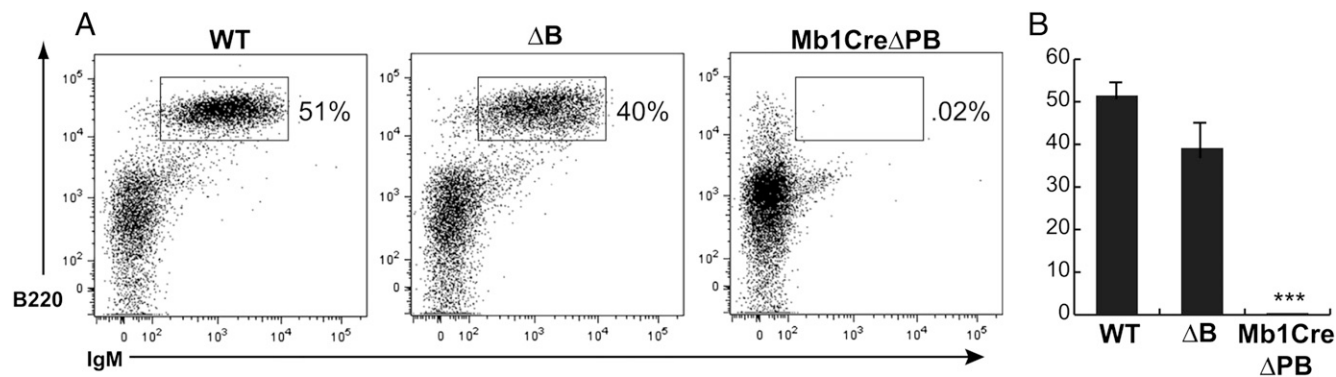


FIGURE 1. Absence of PU.1 and Spi-B during B cell development severely impairs B cell maturation. **(A)** Flow cytometric analysis of B220 and IgM cell surface expression of spleen cells prepared from WT (left panel), ΔB (center panel), and Mb1-CreΔPB (right panel) mice. **(B)** Percentage of B220⁺ IgM⁺ cells in WT, ΔB, and Mb1-CreΔPB mice ($n = 7$). Data are mean \pm SEM. *** $p \leq 0.001$.

analysis. Protein-classification analysis showed that 11% of PU.1-upregulated or -downregulated genes encoded proteins related to nucleic acid binding, whereas 7% of upregulated or downregulated genes encoded transcription factors (Fig. 4A). PU.1-regulated genes encoded cell signaling molecules, cell receptors, and cellular transporters, among others, illustrating a broad role for PU.1 in regulating diverse cellular processes (Fig. 4A, 4B). Gene ontology analysis using DAVID showed that upregulated genes were classified into biological processes including immune response, cell activation, and lymphocyte activation (Fig. 4C). Downregulated genes were classified into biological pathways including nucleosome assembly, chromatin assembly, and nucleosome organization (Fig. 4C). These genes included a number of genes previously shown to be directly regulated by PU.1, such as *Blnk* (38), *Il7r* (39), and *E2f1* (40) (Fig. 4B). Interestingly, *Rag1/Rag2* was the fifth most upregulated gene and was associated with an upstream peak in PU.1 interaction (Fig. 4D). *Id2*, an inhibitor of E2A transcription factor activity, was a downregulated gene that was associated with a peak in PU.1 interaction (Fig. 4E). RT-qPCR analysis confirmed upregulation of *Rag1*, *Rag2*, and *Spi1* transcript levels, as well as downregulation of *Id2* mRNA transcript levels (Fig. 4F). These results suggest that PU.1 directly regulates genes involved in BCR signaling, as well as *Ig* recombination and/or accessibility.

Regulation of *Igk* transcription and recombination by PU.1

Upregulation of *Rag* mRNA transcripts and downregulation of *Id2* mRNA transcripts suggested that PU.1 may be involved in the regulation of *Igk* rearrangement during B cell development. *Igk* V-J rearrangement is preceded by increased transcription of V region genes, as well as of sterile transcripts initiating in regulatory regions (9, 41). Analysis of ChIP-seq data identified 179 peaks in PU.1 interaction within the 3-Mb *Igk* locus, of which 60 were located in GENCODE-annotated *Igk* genes (Fig. 5A). Analysis of RNA-seq data revealed widespread changes in *Igk* V region mRNA transcript levels upon PU.1 induction (Fig. 5B). For 166 annotated *Igk* genes, 69 were unchanged, 42 were downregulated, and 55 were upregulated in the RNA-seq analysis (Fig. 5B, Supplemental Table III). Thirty peaks in PU.1 interaction were associated with increased upregulated *Igk* V transcripts, and 10 peaks in PU.1 interaction were associated with downregulated *Igk* V transcripts (Fig. 5A). *Igk* V genes that were upregulated upon PU.1 induction included *Igkv1-135*, *Igkv10-96*, *Igkv4-57*, *Igkv6-13*, and *Igkv4-73* (Fig. 5B). Each of these *Igk* V genes was associated with at least one peak in PU.1 interaction (Fig. 5C, left panels). Quantitative PCR analysis confirmed that each of these *Igk* V genes was inducible by PU.1, and reduced IL-7 concen-

tration resulted in increased induction of transcription by PU.1 (Fig. 5C, right panels). PU.1 also was shown to interact with the 2-4 and 3-1 enhancers in the *Igλ* locus (42). Interestingly, induction of PU.1 increased *Igλ1* mRNA transcript levels (Fig. 5D). These results suggest that PU.1 directly regulates *Igκ* and *Igλ* V region transcription in i660BM cells.

Interestingly, there were two distinct patterns of PU.1 interaction with *Ig* V genes. PU.1 interacted with the promoters of 11 V genes, with a region downstream of the second exon of 26 V genes, and with both the promoter and a region downstream of the second exon of 14 genes (Fig. 5E, Supplemental Table IV). For the *Igkv4* family, PU.1 interacted with 11 sites downstream of the second exon and only one site in a promoter. For the *Igkv6* family, PU.1 interacted with both the promoter and a site downstream of the second exon for six members (Fig. 5C, 5F). A total of 32 of 40 PU.1 sites downstream of V region second exons were located an average of 91 bp from the RSS heptamer sequence 5'-CACAGTG-3'. MEME analysis of the 32 genomic regions associated with PU.1 binding sites located downstream of V region second exons revealed a 12-bp RSS as the most frequently discovered motif (Fig. 5G). The PU.1 motif was also enriched in these sequences (data not shown). Taken together, these results indicate that PU.1 interacts with a number of sites downstream of *Igk* V region second exons that are located close to RSSs. This suggests that PU.1 might be involved in the regulation of chromatin accessibility near RSSs.

Because PU.1 interacts with *Igk* V region genes, induces *Igk* V region transcription, and induces *Rag* transcription, we hypothesized that PU.1 induction in i660BM cells coupled with reduced IL-7 concentration might be sufficient to induce *Igk* V-J rearrangement in i660BM cells. To confirm this, *Igk* V-J rearrangement was measured using DNA prepared from i660BM cells in which PU.1 was induced with doxycycline in the presence of a high or low concentration of IL-7. DNA prepared from WT spleen cells was used as a control (Fig. 5H, right side). Low IL-7 concentration or PU.1 induction resulted in low levels of *Igk* V-J rearrangement in i660BM cells (Fig. 5H, left side). *Igk* V-J rearrangement was robustly detected in i660BM cells in which PU.1 was induced with a low concentration of IL-7 (Fig. 5H, left side). In parent 660BM cells that did not express PU.1, reduced IL-7 concentration was not sufficient to induce *Igk* V-J rearrangement (Fig. 5H, right side). We conclude that induction of PU.1 expression, coupled with reduced IL-7 concentration, is sufficient to induce *Igk* V-J rearrangement in a cultured pro-B cell line.

Reduced *Igk* transcription in BM pre-B cells from Mb1-CreΔPB mice

Igk V gene transcription is upregulated during the large pre-B (fraction C) to small pre-B (fraction D) transition (43). BM

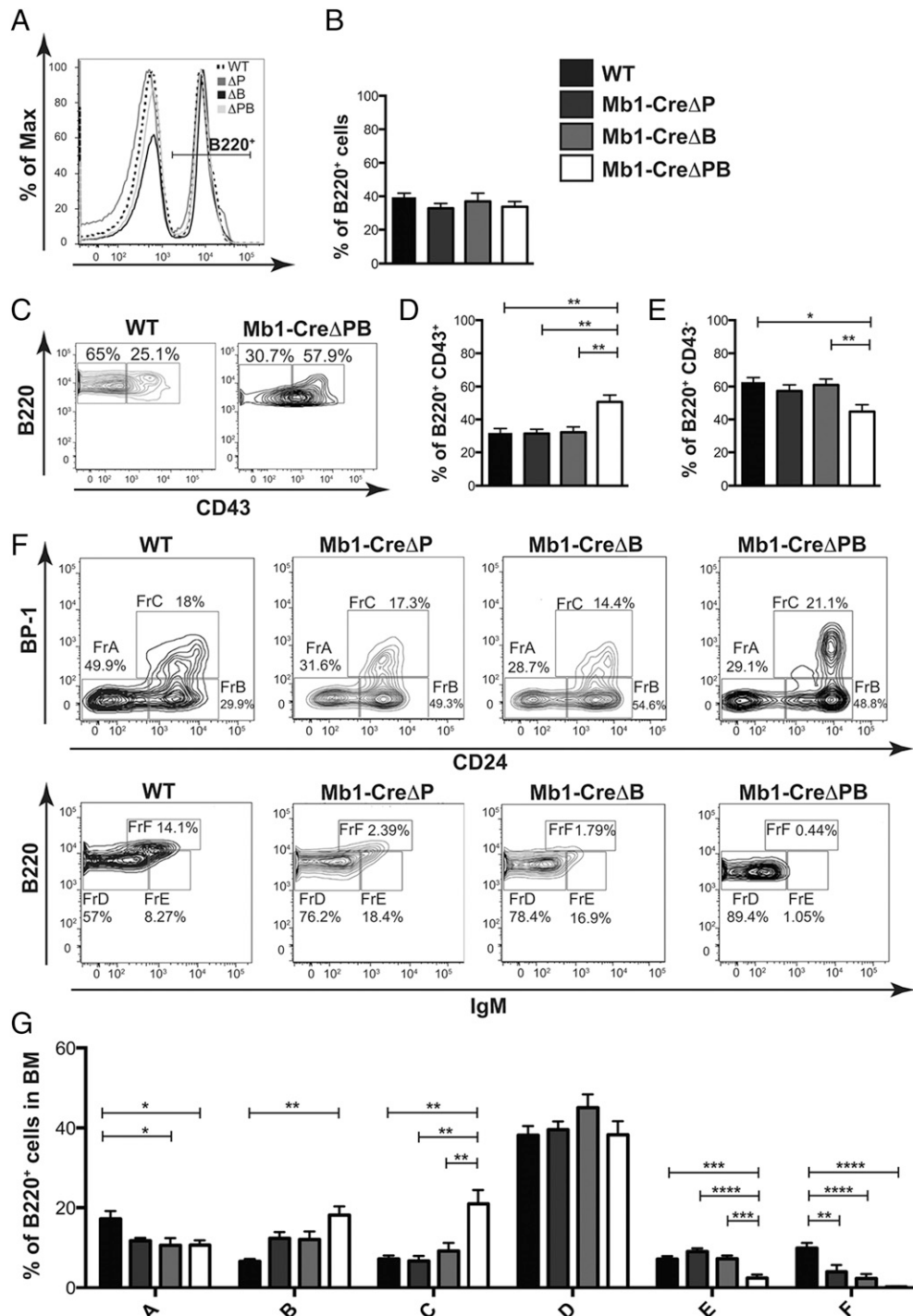
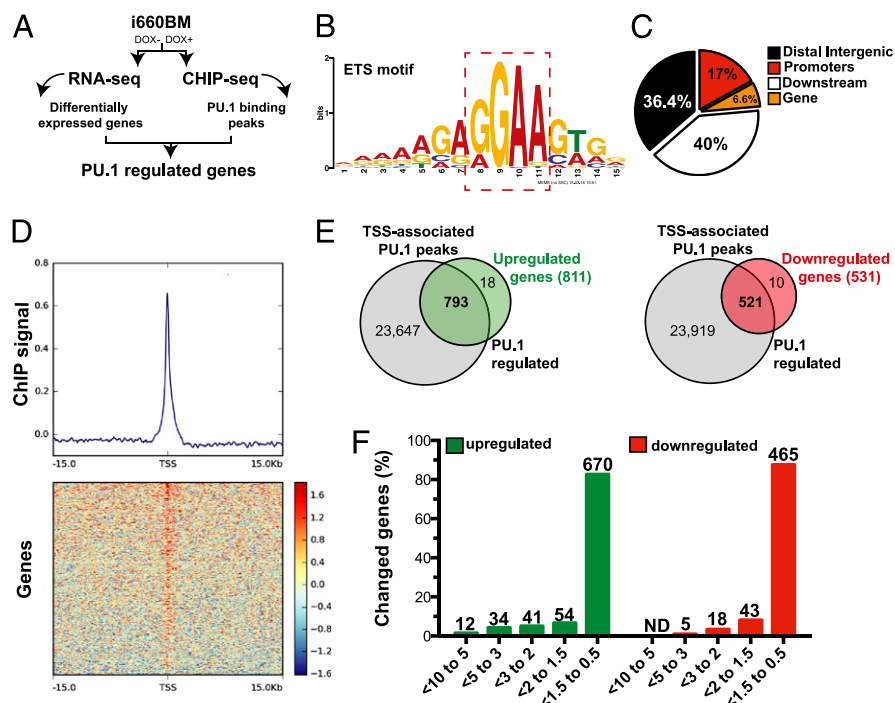


FIGURE 2. Deletion of PU.1 and Spi-B blocks B cell development in the BM at the pre-B cell transition. (A) Representative graph showing the percentage of B220⁺ cells in WT, Mb1-CreΔP, ΔB, and Mb1-CreΔPB mice. (B) Percentage of B220⁺ cells in BM of WT, Mb1-CreΔP, ΔB, and Mb1-CreΔPB mice. (C) Representative flow cytometric analysis showing the percentage of B220⁺ CD43⁻ and B220⁺ CD43⁺ cells in WT (left panel) and Mb1-CreΔPB (right panel) mice. (D) Percentage of B220⁺ CD43⁺ cells in BM of WT, Mb1-CreΔP, ΔB, and Mb1-CreΔPB mice. (E) Percentage of B220⁺ CD43⁻ cells in BM of WT, Mb1-CreΔP, ΔB, and Mb1-CreΔPB mice. (F) Representative flow cytometric analysis according to the Hardy scheme representing the frequency of developing B cells in fractions A–C in WT, Mb1-CreΔP, ΔB, and Mb1-CreΔPB mice (gated on B220⁺ CD43⁺ population) (upper panels). Flow cytometric analysis according to the Hardy scheme representing the frequency of developing B cells in fractions D–F in WT, Mb1-CreΔP, ΔB, and Mb1-CreΔPB mice (gated on B220⁺ CD43⁻ population) (lower panels). (G) Percentage of B220⁺ cells in BM of WT, Mb1-CreΔP, ΔB, and Mb1-CreΔPB mice in fractions (A–F). WT, $n = 10$; Mb1-CreΔP, $n = 8$; ΔB, $n = 9$; and Mb1-CreΔPB, $n = 12$. Data are mean \pm SEM. * $p \leq 0.05$, ** $p \leq 0.01$, *** $p \leq 0.001$, **** $p \leq 0.0001$.

B cell development was blocked at the small pre-B cell stage in the absence of PU.1 and Spi-B (Fig. 1). Because induction of PU.1 resulted in increased *Igk* V region transcript levels and *Igk* V-J recombination, we hypothesized that Mb1-CreΔPB pre-B cells might have a reduced ability to activate *Igk* V-J transcription.

To test this, fraction C and fraction D pre-B cells were enriched from the BM of Mb1-CreΔPB mice, or ΔB mice as controls, using cell sorting; the gating strategy is shown in Fig. 2F. Fraction E cells were not enriched, because this fraction was absent in Mb1-CreΔPB mice (Fig. 2G). Quantitative PCR was used to determine

FIGURE 3. Identification of PU.1-regulated genes in i660BM pro-B cells. **(A)** Flow chart illustrating the strategy used to identify PU.1-regulated genes. RNA-seq of i660BM cells in the presence (+DOX) or absence (–DOX) of doxycycline was integrated with PU.1 ChIP-seq data sets to determine PU.1-regulated genes. Differentially expressed genes in the RNA-seq were categorized by the presence or absence of PU.1 binding within 15 kb of the TSS. **(B)** Motif enrichment analysis of PU.1 ChIP-seq data shows the ETS binding motif as the primary motif of PU.1 binding. **(C)** Pie chart representing the enrichment of PU.1 binding across genomic regions based on PU.1 ChIP-seq analysis. **(D)** Clustering of PU.1 ChIP-seq data demonstrates PU.1-enriched regions at the TSS of mouse RefSeq genes. **(E)** Defining PU.1-regulated genes. Venn diagrams illustrate the number of TSS-associated PU.1 peaks associated with upregulated (left panel; green circle) and downregulated (right panel; red circle) genes from the RNA-seq experiment. **(F)** Distribution of PU.1-regulated genes according to RNA-seq fold change (\log_2).



changes in transcript levels of *Igk* V genes with which PU.1 interacted. We found that, in BM cells from ΔB mice, *Igk* V gene transcription was upregulated during the fraction C to fraction D transition for *Igkv1-135*, *Igkv12-98*, *Igkv12-44*, *Igkv3-5*, and the sterile transcript *Gkl-1* (Fig. 6A–F). In contrast, transcript levels for *Btk* and the control gene β -actin did not change (Fig. 6G, 6H). In BM cells enriched from Mb1-Cre Δ PB mice, mRNA transcript levels for *Igkv1-135*, *Igkv12-98*, *Igkv12-44*, *Igkv3-5*, and *Gkl-1* failed to increase during the fraction C to fraction D transition (Fig. 6B–F). Transcript levels for *Spi1* and its target gene (*Btk*) decreased, consistent with deletion of *Spi1* at this transition, whereas the control gene β -actin did not change from fraction C to fraction D (Fig. 6G–I). These data demonstrate that PU.1 and Spi-B are important for inducing transcription of certain *Igk* V genes during B cell development in the BM and suggest that the absence of PU.1 and Spi-B might lead to reduced *Igk* V region accessibility and V–J recombination.

Discussion

In this study, we showed that B cell development is blocked in mice that delete the *Spi1* gene encoding PU.1 under control of the *Mb1* locus, which are also germline knockout for *Spib* (Mb1-Cre Δ PB mice). Adult Mb1-Cre Δ PB mice did not have splenic B cells, and few surface IgM⁺ B cells were present in BM, suggesting a block in B cell development starting at the pre-B cell stage. Identifying target genes of PU.1 and/or Spi-B might explain this block in B cell development; therefore a *Spi1*/*Spib*-deleted IL-7-dependent pro-B cell line was used in which PU.1 expression can be induced using doxycycline (i660BM cells). RNA-seq and anti-PU.1 ChIP-seq experiments were performed to determine the genome-wide target genes of PU.1 in this model. These experiments confirmed a number of previously identified PU.1 target genes involved in the pro-B to pre-B cell developmental transition. Unexpectedly, the *Rag* locus was also found to be a direct target of PU.1 induction. Closer examination revealed that PU.1 interacted with 179 sites within the *Igk* locus, of which 60 sites were located within V genes, including at V gene promoters and near RSSs. An increase in PU.1 expression, combined with reduced IL-7 concentration, induced *Igk*

rearrangement. Finally, we found that *Igk* V region mRNA transcript levels were not increased at the pro-B to pre-B cell transition in Mb1-Cre Δ PB mice. These results show that PU.1 directly regulates *Igk* locus transcription and suggest that PU.1 is an important regulator of *Igk* locus accessibility during B cell development.

Comparison of BM B cell development in Mb1-Cre Δ PB mice with that in control mice revealed a relative increase in the frequency of pre-BII/large pre-B cells (fraction C), no difference in the frequency of small pre-B cells (fraction D), and a near absence of immature sIgM⁺ B cells (fraction E). These results are most consistent with a block in B cell development at the stage when *Ig* L chain recombination is taking place in small pre-B cells. Previous analysis of CD19-Cre Δ PB mice, which did not delete alleles efficiently in BM, showed a relative increase in immature B cell frequencies in BM but a decrease in mature recirculating B cells (fraction F) and in the frequency of splenic follicular B cells. The differences between these two models suggest that PU.1 and Spi-B play important roles in B cell development at late, as well as early, stages.

B cell-specific deletion of the gene encoding PU.1 in mice (34, 35) or deletion of the gene encoding Spi-B in mice (44) resulted in relatively mild defects in B cell development. Similarly, deletion of the *Irf4* or *Irf8* gene resulted in mild B cell developmental defects (45, 46). Combined deletion of *Spi1* and *Irf8* resulted in mild impairment of B cell development, whereas combined deletion of *Spi1* and *Irf4* resulted in impaired B cell development at the pre-B cell stage (36). Strikingly, combined deletion of *Irf4* and *Irf8* resulted in a block in B cell development at the pre-B cell stage (47). In this study, we showed that combined deletion of *Spi1* and *Spib* results in a block in B cell development at the pre-B cell stage. Collectively, these studies reveal a critically important PU.1/Spi-B/IRF4/IRF8 regulatory axis for pre-B cell development. PU.1 and Spi-B interact interchangeably with IRF4 or IRF8 to regulate genes containing ETS-IRF composite elements (EICEs) (48). Recently, it was shown that ~50% of PU.1 binding sites in pro-B cells are at EICEs, suggesting that this regulatory element may control a large number of genes in developing B cells (36). These studies collectively suggest that genes important for early B cell development require activation through EICEs to

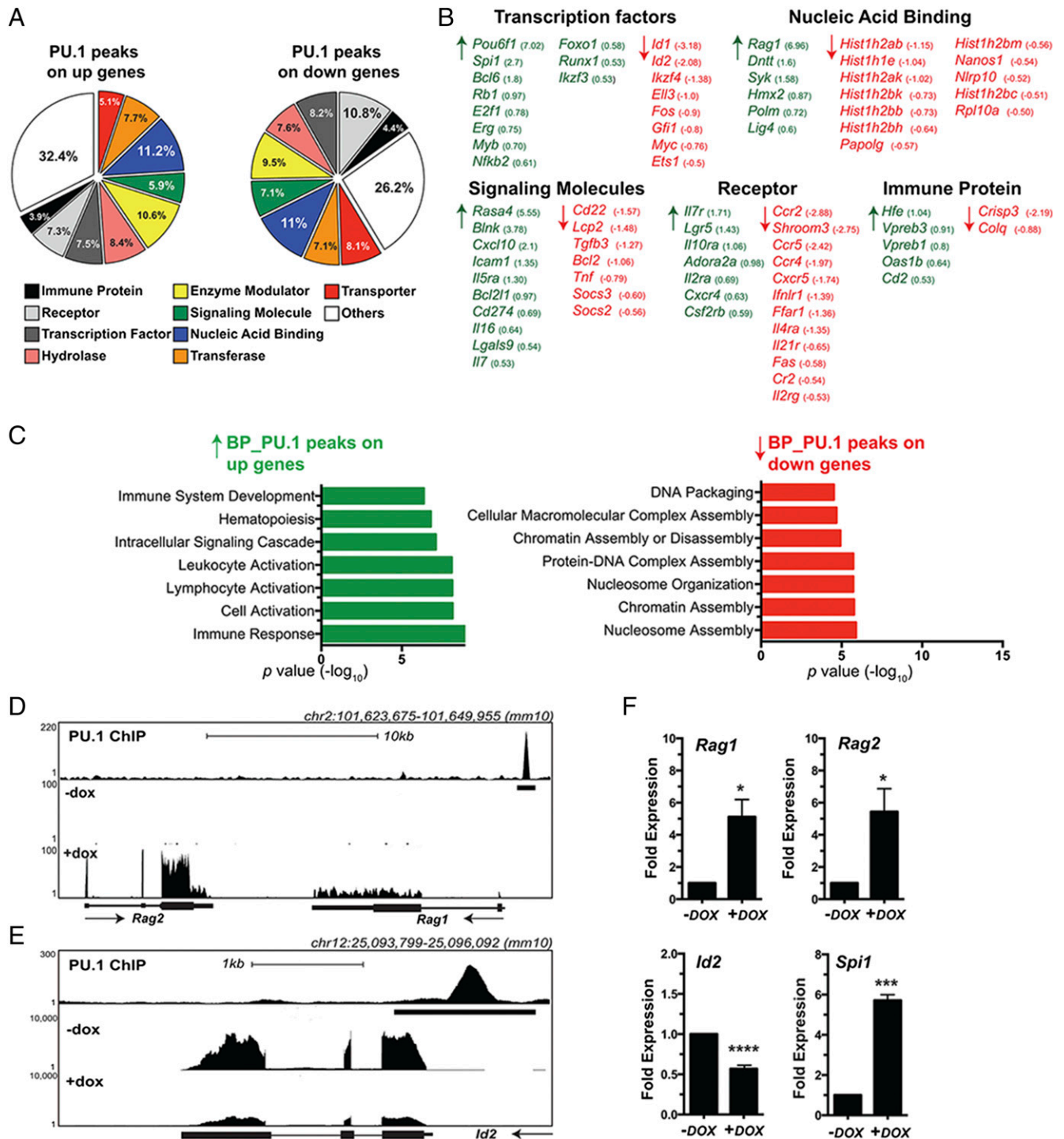


FIGURE 4. Characterization of PU.1-regulated genes. **(A)** Gene ontology data analysis showing the PANTHER protein classification of PU.1-regulated genes (left panel, upregulated; right panel, downregulated). **(B)** Examples of PU.1-upregulated (\uparrow) and downregulated (\downarrow) genes according to the protein classification ontology analysis. Numbers indicate \log_2 fold change. **(C)** Gene ontology analysis by DAVID identifying the biological processes related to PU.1-regulated genes (left panel, upregulated; right panel, downregulated). **(D)** UCSC genome browser tracks of PU.1 ChIP and RNA-seq experiments showing *Rag2* and *Rag1* genes. **(E)** UCSC genome browser tracks of PU.1 ChIP and RNA-seq experiments showing *Id2* gene. **(F)** Confirmation of changes in gene expression. RT-qPCR analysis for the indicated genes was performed on four biological replicates of RNA prepared from uninduced (–DOX) or 70 ng/ml doxycycline-induced (+DOX) i660BM cells cultured in 2.5% IL-7-conditioned medium. * $p \leq 0.05$, *** $p \leq 0.001$, **** $p \leq 0.0001$.

promote their expression. More work is necessary to identify key EICE-regulated target genes.

PU.1 was implicated in the regulation of *Ig* transcription in numerous studies. In 1991, PU.1 was recognized to interact with the *Igk* 3' enhancer cooperatively with IRF4 (15, 49). Transgenic studies implicated the PU.1 binding site in the *Igk* 3' enhancer in

the regulation of the developmental stage specificity of V-J joining (50). In 1995, PU.1 was identified as an NF capable of interacting with pyrimidine-rich sequences in the *Vk19* promoter (14). PU.1 binding sites were predicted in numerous V region promoters of the *Igk* locus (16). Previous studies showed that PU.1 interacts with numerous sites in the *Igk* locus in the B cell lineage. In

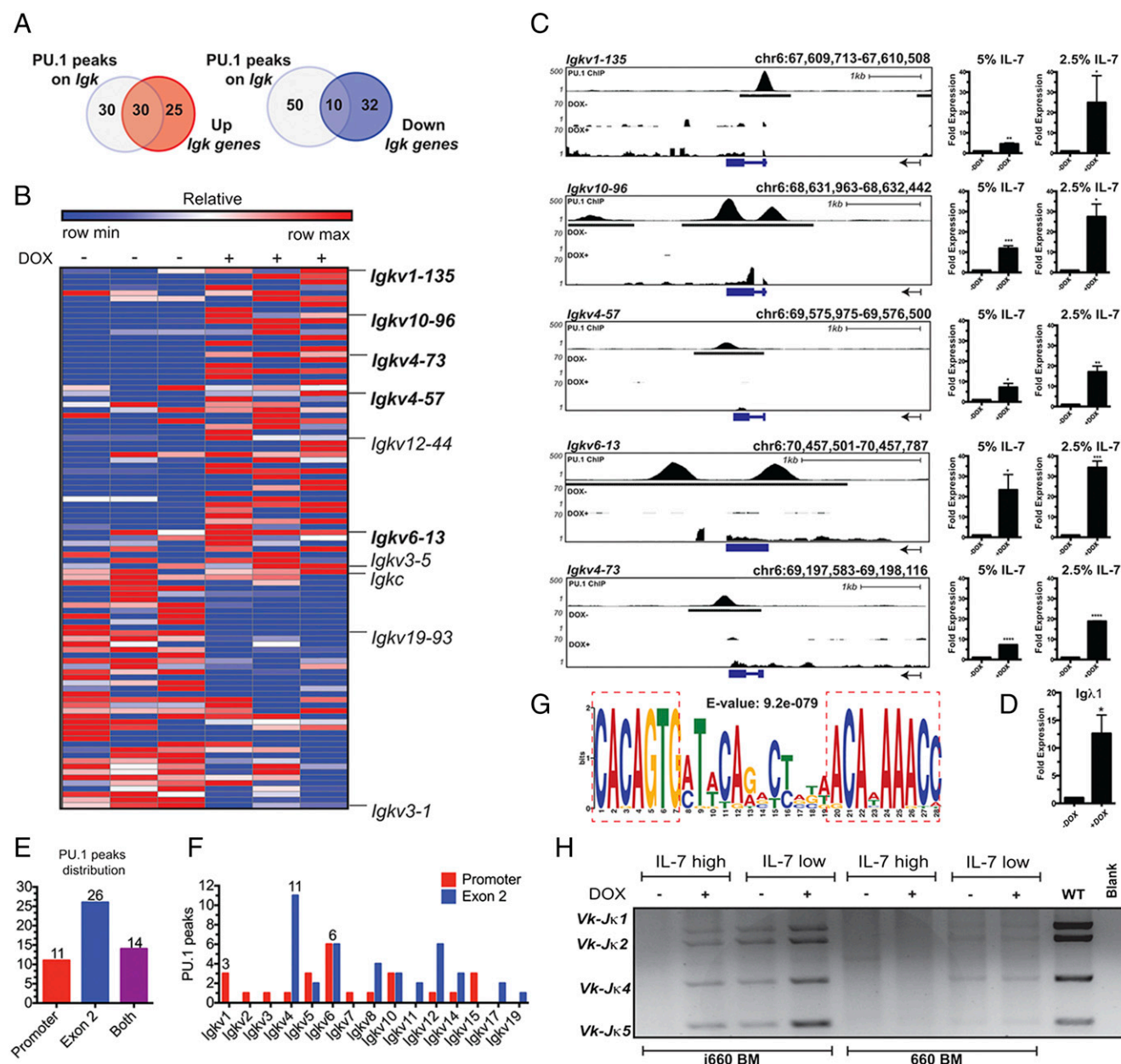


FIGURE 5. PU.1 induction in i660BM pro-B cells induces transcription and rearrangement of the *Igκ* locus. **(A)** Venn diagrams showing the number of PU.1 peaks located on upregulated and downregulated *Igκ* V genes. **(B)** Heat map showing the differential expression of *Igκ* V genes with (+DOX) or without (−DOX) doxycycline using the mouse genome annotation available on GENCODE. **(C)** RT-qPCR for detection of *Igkv* 1-135, *Igkv10-96*, *Igkv4-57*, *Igkv6-13*, and *Igkv4-73* transcripts with (+DOX) or without (−DOX) doxycycline in 5 and 2.5% of IL-7. UCSC genome tracks (left panels) show the PU.1 binding peak from PU.1 ChIP-seq data and the transcription tracks from the RNA-seq experiment in conditions without (−DOX) and with (+DOX) doxycycline. **(D)** PU.1 induces *Igλ* germline transcription. RT-qPCR analysis of the *Igλ1* mRNA transcript was performed on four biological replicates of RNA prepared from uninduced (−DOX) or 70 ng/ml doxycycline-induced (+DOX) i660BM cells cultured in 2.5% IL-7–conditioned medium. **(E)** Distribution of PU.1 peaks within the *Igκ* V locus. **(F)** Distribution of PU.1 peaks separated by *Igκ* V family. **(G)** MEME motif analysis of sequences containing PU.1 peaks downstream of *Igκ* V gene second exons show RSS as a top enriched motif. **(H)** PCR for detection of *Igκ*-chain rearrangement (*Igkvκ-Igk5*) in i660BM and 660BM cells without doxycycline (−DOX) and with doxycycline (+DOX) induction and various levels of IL-7. * $p \leq 0.05$, ** $p \leq 0.01$, *** $p \leq 0.001$, **** $p \leq 0.0001$.

mature splenic B cells, PU.1 was shown to interact with 45 sites in the 3-Mb *Igκ* locus (37). In pro-B cells, PU.1 was shown to interact with 181 sites in the *Igκ* locus (17). This study closely agrees with our result of 179 total PU.1 binding sites in the *Igκ* locus, and 74 of these sites were in common, with 35 of these sites in common in all three studies. Taken together, these studies correspond with our identification of PU.1 binding sites in the *Igκ* locus.

The 3' enhancer of the *Igκ* locus is critical for the cell type and developmental stage specificity of V-J rearrangement (10, 50–52). STAT5 binding induced by IL-7 signaling is a critically

important repressor of *Igκ* transcription to prevent accessibility and rearrangement during proliferation of large pre-B/pre-BII cells (53). PU.1 can compete with STAT5 for interaction with the *Igκ* 3' enhancer to regulate *Igκ* transcription (54). Consistent with these studies, our results showed that PU.1 induced *Igκ* transcription and rearrangement more efficiently when IL-7 concentration was reduced (Fig. 5). Our results are consistent with PU.1 being an important factor for inducing *Igκ* transcription and accessibility when developing pre-B cells migrate away from high IL-7 concentrations (55).

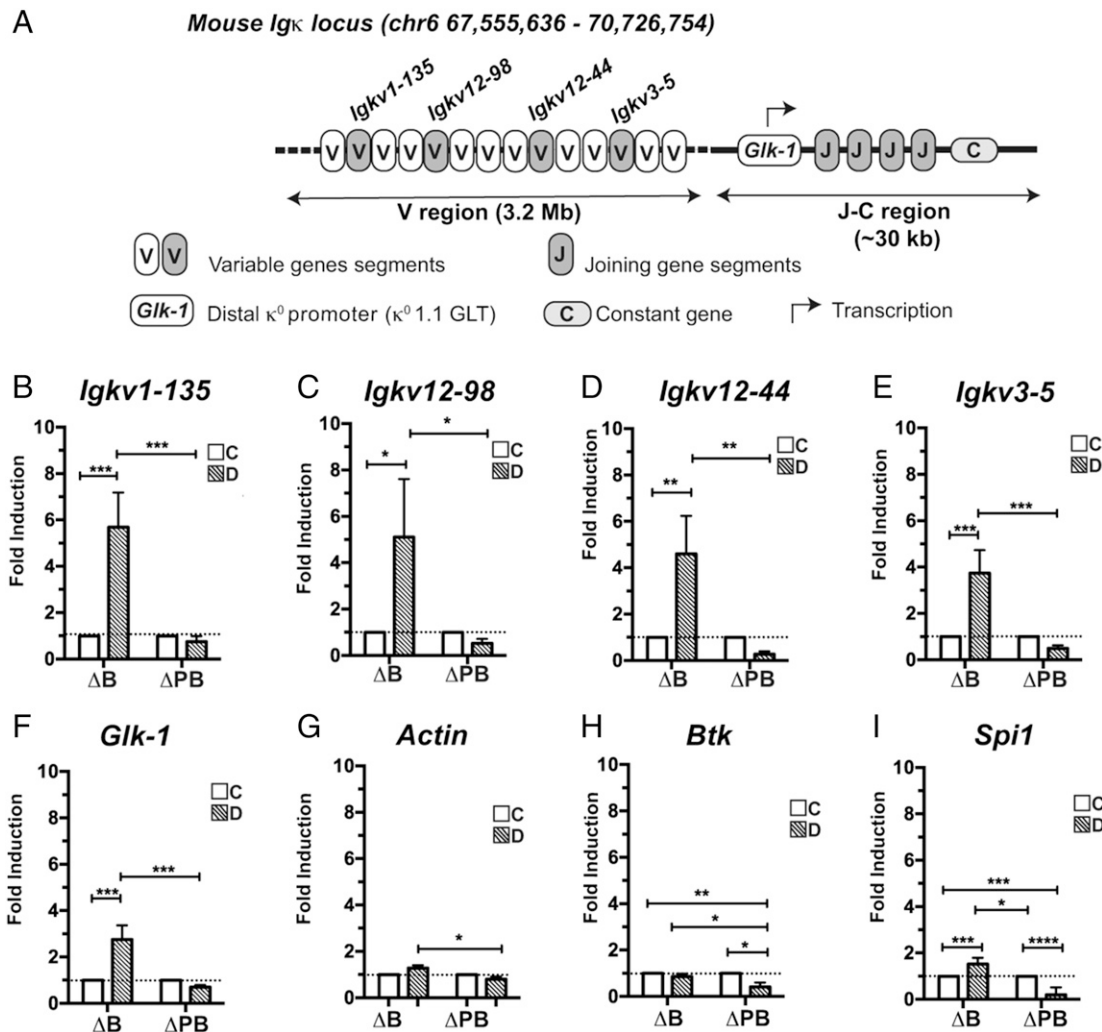


FIGURE 6. Absence of PU.1 and Spi-B in vivo results in reduced levels of *Igκ* transcripts in small pre-B cells. **(A)** Schematic diagram of the mouse *Igκ* locus showing the variable (V) region, the joining and constant regions (C-V regions), and the gene segments assessed in this study by RT-qPCR. Variable gene segments are highlighted, and the *Glk-1* (κ^0) transcript is also indicated. **(B–E)** RT-qPCR showing the fold induction of the *Igkv1-135*, *Igkv12-98*, *Igkv12-44*, and *Igkv3-5* genes in developing B cells from fraction C (large pre-B cells) and fraction D (small pre-B cells) of ΔB and Mb1-CreΔPB mouse BM. **(F)** RT-qPCR showing the fold induction of the *Glk-1* mRNA transcript in developing B cells from fraction C (large pre-B cells) and fraction D (small pre-B cells) of ΔB and Mb1-CreΔPB mouse BM. **(G–I)** RT-qPCR showing the fold induction of *βactin*, *Btk*, and *Spi1* mRNA transcripts in developing B cells from fraction C (large pre-B cells) and fraction D (small pre-B cells) of ΔB and Mb1-CreΔPB mouse BM. * $p \leq 0.05$, ** $p \leq 0.01$, *** $p \leq 0.001$, **** $p \leq 0.0001$.

Igκ V region transcription is closely associated with accessibility of the recombinase apparatus and initiation of *Igκ* V-J recombination (9, 41). The results presented in Fig. 6 demonstrate that *Igκ* V region transcripts are not appropriately upregulated in the absence of PU.1 and Spi-B. This suggests that PU.1 and Spi-B are important regulators of *Igκ* V region transcription, accessibility, and rearrangement. The absence of IgM⁺ B cells in Mb1-CreΔPB mice suggests that *Igλ* transcription may also be impaired in the absence of PU.1 and Spi-B. Consistent with this idea, induction of PU.1 activated *Igλ1* transcription in i660BM cells (Fig. 5D). We previously demonstrated that *Igλ* transcription was reduced in PU.1/Spi-B double-knockout pro-B cell lines (56). In summary, we expect that reduced *Igκ* V region transcription in fraction D small pre-B cells lacking PU.1 and Spi-B results in impaired *Igκ* V region accessibility and impaired *Igκ* recombination, which lead to a block in B cell development at the small pre-B cell stage. These studies reveal an important role for PU.1 in *Igκ* transcription and rearrangement, as well as a requirement for PU.1 and Spi-B in B cell development.

Acknowledgments

We thank Michael Reth (Freiburg, Germany) and John Weis (University of Utah) for providing Mb1-Cre mice. We thank scientists and staff of the McGill University and Génome Québec Innovation Centre for performing library construction and next-generation sequencing. We also thank Kristin Chadwick and the London Regional Flow Cytometry Core Facility for assistance with flow cytometric sorting and analysis.

Disclosures

The authors have no financial conflicts of interest.

References

- Lu, L., G. Smithson, P. W. Kincade, and D. G. Osmond. 1998. Two models of murine B lymphopoiesis: a correlation. *Eur. J. Immunol.* 28: 1755–1761.
- Osmond, D. G., A. Rolink, and F. Melchers. 1998. Murine B lymphopoiesis: towards a unified model. *Immunol. Today* 19: 65–68.
- Hardy, R. R., C. E. Carmack, S. A. Shinton, J. D. Kemp, and K. Hayakawa. 1991. Resolution and characterization of pro-B and pre-pro-B cell stages in normal mouse bone marrow. *J. Exp. Med.* 173: 1213–1225.

4. Teng, G., Y. Maman, W. Resch, M. Kim, A. Yamane, J. Qian, K. R. Kieffer-Kwon, M. Mandal, Y. Ji, E. Meffre, et al. 2015. RAG represents a widespread threat to the lymphocyte genome. *Cell* 162: 751–765.
5. Corfe, S. A., and C. J. Paige. 2009. Development of B lymphocytes. In *Molecular Basis of Hematopoiesis*. A. Wickrema, and B. L. Kee, eds. Springer, New York, p. 173–199.
6. Allman, D., R. C. Lindsley, W. DeMuth, K. Rudd, S. A. Shinton, and R. R. Hardy. 2001. Resolution of three nonproliferative immature splenic B cell subsets reveals multiple selection points during peripheral B cell maturation. *J. Immunol.* 167: 6834–6840.
7. Aoki-Ota, M., A. Torkamani, T. Ota, N. Schork, and D. Nemazee. 2012. Skewed primary Igk repertoire and V-J joining in C57BL/6 mice: implications for recombination accessibility and receptor editing. *J. Immunol.* 188: 2305–2315.
8. Ribeiro de Almeida, C., R. W. Hendriks, and R. Stadhouders. 2015. Dynamic control of long-range genomic interactions at the immunoglobulin κ light-chain locus. *Adv. Immunol.* 128: 183–271.
9. Yancopoulos, G. D., and F. W. Alt. 1985. Developmentally controlled and tissue-specific expression of unrearranged VH gene segments. *Cell* 40: 271–281.
10. Inlay, M., F. W. Alt, D. Baltimore, and Y. Xu. 2002. Essential roles of the kappa light chain intronic enhancer and 3' enhancer in kappa rearrangement and demethylation. *Nat. Immunol.* 3: 463–468.
11. Sleckman, B. P., J. R. Gorman, and F. W. Alt. 1996. Accessibility control of antigen-receptor variable-region gene assembly: role of cis-acting elements. *Annu. Rev. Immunol.* 14: 459–481.
12. Pang, S. H., S. Carotta, and S. L. Nutt. 2014. Transcriptional control of pre-B cell development and leukemia prevention. *Curr. Top. Microbiol. Immunol.* 381: 189–213.
13. Solomon, L. A., S. K. Li, J. Piskorz, L. S. Xu, and R. P. DeKoter. 2015. Genome-wide comparison of PU.1 and Spi-B binding sites in a mouse B lymphoma cell line. *BMC Genomics* 16: 76.
14. Schwarzenbach, H., J. W. Newell, and P. Matthias. 1995. Involvement of the Ets family factor PU.1 in the activation of immunoglobulin promoters. *J. Biol. Chem.* 270: 898–907.
15. Pongubala, J. M., and M. L. Atchison. 1991. Functional characterization of the developmentally controlled immunoglobulin kappa 3' enhancer: regulation by Id, a repressor of helix-loop-helix transcription factors. *Mol. Cell. Biol.* 11: 1040–1047.
16. Brekke, K. M., and W. T. Garrard. 2004. Assembly and analysis of the mouse immunoglobulin kappa gene sequence. *Immunogenetics* 56: 490–505.
17. Schwickert, T. A., H. Tagoh, S. Gültekin, A. Dakic, E. Axelsson, M. Minnich, A. Ebert, B. Werner, M. Roth, L. Cimmino, et al. 2014. Stage-specific control of early B cell development by the transcription factor Ikaros. *Nat. Immunol.* 15: 23–293.
18. Sokalski, K. M., S. K. Li, I. Welch, H. A. Cadieux-Pitre, M. R. Gruca, and R. P. DeKoter. 2011. Deletion of genes encoding PU.1 and Spi-B in B cells impairs differentiation and induces pre-B cell acute lymphoblastic leukemia. *Blood* 118: 2801–2808.
19. Christie, D. A., L. S. Xu, S. A. Turkistany, L. A. Solomon, S. K. Li, E. Yim, I. Welch, G. I. Bell, D. A. Hess, and R. P. DeKoter. 2015. PU.1 opposes IL-7-dependent proliferation of developing B cells with involvement of the direct target gene bruton tyrosine kinase. *J. Immunol.* 194: 595–605.
20. Hobeika, E., S. Thiemann, B. Storch, H. Jumaa, P. J. Nielsen, R. Pelanda, and M. Reth. 2006. Testing gene function early in the B cell lineage in mb1-cre mice. *Proc. Natl. Acad. Sci. USA* 103: 13789–13794.
21. Winkler, T. H., A. Rolink, F. Melchers, and H. Karasuyama. 1995. Precursor B cells of mouse bone marrow express two different complexes with the surrogate light chain on the surface. *Eur. J. Immunol.* 25: 446–450.
22. Trapnell, C., A. Roberts, L. Goff, G. Pertea, D. Kim, D. R. Kelley, H. Pimentel, S. L. Salzberg, J. L. Rinn, and L. Pachter. 2012. Differential gene and transcript expression analysis of RNA-seq experiments with TopHat and Cufflinks. *Nat. Protoc.* 7: 562–578.
23. Afgan, E., D. Baker, M. van den Beek, D. Blankenberg, D. Bouvier, M. Čech, J. Chilton, D. Clements, N. Coraor, C. Eberhard, et al. 2016. The galaxy platform for accessible, reproducible and collaborative biomedical analyses: 2016 update. *Nucleic Acids Res.* 44(W1): W3–W10.
24. Huang da, W., B. T. Sherman, and R. A. Lempicki. 2009. Systematic and integrative analysis of large gene lists using DAVID bioinformatics resources. *Nat. Protoc.* 4: 44–57.
25. Mi, H., A. Muruganujan, J. T. Casagrande, and P. D. Thomas. 2013. Large-scale gene function analysis with the PANTHER classification system. *Nat. Protoc.* 8: 1551–1566.
26. Langmead, B., C. Trapnell, M. Pop, and S. L. Salzberg. 2009. Ultrafast and memory-efficient alignment of short DNA sequences to the human genome. *Genome Biol.* 10: R25.
27. Shin, H., T. Liu, A. K. Manrai, and X. S. Liu. 2009. CEAS: cis-regulatory element annotation system. *Bioinformatics* 25: 2605–2606.
28. Ramirez, F., F. Dündar, S. Diehl, B. A. Grüning, and T. Manke. 2014. Deeptools: a flexible platform for exploring deep-sequencing data. *Nucleic Acids Res.* 42: W187–W191.
29. Harrow, J., F. Denoeud, A. Frankish, A. Reymond, C. K. Chen, J. Chrast, J. Lagarde, J. G. Gilbert, R. Storey, D. Swarbreck, et al. 2006. GENCODE: producing a reference annotation for ENCODE. *Genome Biol.* 7 (Suppl. 1): S4.1–S4.9.
30. Quinlan, A. R., and I. M. Hall. 2010. BEDTools: a flexible suite of utilities for comparing genomic features. *Bioinformatics* 26: 841–842.
31. Heberle, H., G. V. Meirelles, F. R. da Silva, G. P. Telles, and R. Minghim. 2015. InteractiVenn: a web-based tool for the analysis of sets through Venn diagrams. *BMC Bioinformatics* 16: 169.
32. Cobaleda, C., W. Jochum, and M. Busslinger. 2007. Conversion of mature B cells into T cells by dedifferentiation to uncommitted progenitors. *Nature* 449: 473–477.
33. Livak, K. J., and T. D. Schmittgen. 2001. Analysis of relative gene expression data using real-time quantitative PCR and the 2^{(-Delta Delta C(T))} method. *Methods* 25: 402–408.
34. Polli, M., A. Dakic, A. Light, L. Wu, D. M. Tarlinton, and S. L. Nutt. 2005. The development of functional B lymphocytes in conditional PU.1 knock-out mice. *Blood* 106: 2083–2090.
35. Ye, M., O. Ermakova, and T. Graf. 2005. PU.1 is not strictly required for B cell development and its absence induces a B-2 to B-1 cell switch. *J. Exp. Med.* 202: 1411–1422.
36. Pang, S. H., M. Minnich, P. Gangatirakar, Z. Zheng, A. Ebert, G. Song, R. A. Dickens, L. M. Corcoran, C. G. Mullighan, M. Busslinger, et al. 2016. PU.1 cooperates with IRF4 and IRF8 to suppress pre-B-cell leukemia. *Leukemia* 30: 1375–1387.
37. Heinz, S., C. Benner, N. Spann, E. Bertolino, Y. C. Lin, P. Laslo, J. X. Cheng, C. Murte, H. Singh, and C. K. Glass. 2010. Simple combinations of lineage-determining transcription factors prime cis-regulatory elements required for macrophage and B cell identities. *Mol. Cell* 38: 576–589.
38. Xu, L. S., K. M. Sokalski, K. Hotke, D. A. Christie, O. Zarnett, J. Piskorz, G. Thillainadesan, J. Torchia, and R. P. DeKoter. 2012. Regulation of B cell linker protein transcription by PU.1 and Spi-B in murine B cell acute lymphoblastic leukemia. *J. Immunol.* 189: 3347–3354.
39. DeKoter, R. P., B. L. Schweitzer, M. B. Kamath, D. Jones, H. Tagoh, C. Bonifer, D. A. Hildeman, and K. J. Huang. 2007. Regulation of the interleukin-7 receptor alpha promoter by the Ets transcription factors PU.1 and GA-binding protein in developing B cells. *J. Biol. Chem.* 282: 14194–14204.
40. Ziliotto, R., M. R. Gruca, S. Podder, G. Noel, C. K. Ogle, D. A. Hess, and R. P. DeKoter. 2014. PU.1 promotes cell cycle exit in the murine myeloid lineage associated with downregulation of E2F1. *Exp. Hematol.* 42: 204–217.e1.
41. Schlissel, M. S., and P. Stanhope-Baker. 1997. Accessibility and the developmental regulation of V(D)J recombination. *Semin. Immunol.* 9: 161–170.
42. Eisenbeis, C. F., H. Singh, and U. Storb. 1993. PU.1 is a component of a multiprotein complex which binds an essential site in the murine immunoglobulin lambda 2-4 enhancer. *Mol. Cell. Biol.* 13: 6452–6461.
43. Painter, M. W., S. Davis, R. R. Hardy, D. Mathis, and C. Benoist. Immunological Genome Project Consortium. 2011. Transcriptomes of the B and T lineages compared by multiplexed microarray profiling. *J. Immunol.* 186: 3047–3057.
44. Su, G. H., H. M. Chen, N. Muthusamy, L. A. Garrett-Sinha, D. Baunoch, D. G. Tenen, and M. C. Simon. 1997. Defective B cell receptor-mediated responses in mice lacking the Ets protein, Spi-B. *EMBO J.* 16: 7118–7129.
45. Mittrücker, H. W., T. Matsuyama, A. Grossman, T. M. Küding, J. Potter, A. Shahinian, A. Wakeham, B. Patterson, P. S. Ohashi, and T. W. Mak. 1997. Requirement for the transcription factor LSIRF/IRF4 for mature B and T lymphocyte function. *Science* 275: 540–543.
46. Holtschke, T., J. Löhler, Y. Kanno, T. Fehr, N. Giese, F. Rosenbauer, J. Lou, K. P. Knobloch, L. Gabriele, J. F. Waring, et al. 1996. Immunodeficiency and chronic myelogenous leukemia-like syndrome in mice with a targeted mutation of the ICSPB gene. *Cell* 87: 307–317.
47. Lu, R., K. L. Medina, D. W. Lancki, and H. Singh. 2003. IRF-4,8 orchestrate the pre-B-to-B transition in lymphocyte development. *Genes Dev.* 17: 1703–1708.
48. Singh, H., E. Glasmachner, A. B. Chang, and B. Vander Lugt. 2013. The molecular choreography of IRF4 and IRF8 with immune system partners. *Cold Spring Harb. Symp. Quant. Biol.* 78: 101–104.
49. Pongubala, J. M., S. Nagulapalli, M. J. Klemsz, S. R. McKercher, R. A. Maki, and M. L. Atchison. 1992. PU.1 recruits a second nuclear factor to a site important for immunoglobulin kappa 3' enhancer activity. *Mol. Cell. Biol.* 12: 368–378.
50. Hayashi, R., T. Takemori, M. Kodama, M. Suzuki, A. Tsuboi, F. Nagawa, and H. Sakano. 1997. The PU.1 binding site is a cis-element that regulates pro-B/pre-B specificity of V kappa-J kappa joining. *J. Immunol.* 159: 4145–4149.
51. Shaffer, A. L., A. Peng, and M. S. Schlissel. 1997. In vivo occupancy of the kappa light chain enhancers in primary pro- and pre-B cells: a model for kappa locus activation. *Immunity* 6: 131–143.
52. Gorman, J. R., N. van der Stoep, R. Monroe, M. Cogne, L. Davidson, and F. W. Alt. 1996. The Ig(kappa) enhancer influences the ratio of Ig(kappa) versus Ig(lambda) B lymphocytes. *Immunity* 5: 241–252.
53. Mandal, M., S. E. Powers, M. Maischein-Cline, E. T. Bartom, K. M. Hamel, B. L. Kee, A. R. Dinner, and M. R. Clark. 2011. Epigenetic repression of the Igk locus by STAT5-mediated recruitment of the histone methyltransferase Ezh2. *Nat. Immunol.* 12: 1212–1220.
54. Hodawadekar, S., K. Park, M. A. Farrar, and M. L. Atchison. 2012. A developmentally controlled competitive STAT5-PU.1 DNA binding mechanism regulates activity of the Ig κ E3' enhancer. *J. Immunol.* 188: 2276–2284.
55. Clark, M. R., M. Mandal, K. Ochiai, and H. Singh. 2014. Orchestrating B cell lymphopoiesis through interplay of IL-7 receptor and pre-B cell receptor signalling. *Nat. Rev. Immunol.* 14: 69–80.
56. Schweitzer, B. L., and R. P. DeKoter. 2004. Analysis of gene expression and Ig transcription in PU.1/Spi-B-deficient progenitor B cell lines. *J. Immunol.* 172: 144–154.